Organometallics **2000,** *19,* 5575−5581

Syntheses and Structures of New Diruthenatetraborane Complexes Exhibiting Novel Modes of Coordination for a B_2H_5 Fragment: Phosphine-Complexed $[(Cp^*Ru)_2(\mu\text{-}H)(\|\text{-}\mu\text{-}\eta^4\text{-}B_2H_5)(PR_3)]$ ($PR_3 = PMe_3, PMe_2Ph$) and Phosphido-Bridged *nido*-$[(Cp^*Ru)_2(\mu\text{-}PMe_2)(\perp\text{-}\mu\text{-}\eta^4\text{-}B_2H_5)]$[1]

Lourdes N. Pangan, Yasuro Kawano,* and Mamoru Shimoi*

Department of Basic Science, Graduate School of Arts and Sciences, University of Tokyo, Meguro-ku, Tokyo 153-8902, Japan

Received July 3, 2000

Reaction of *nido*-$[(Cp^*Ru)_2(\mu\text{-}H)_2(B_3H_7)]$ (**1**) with tertiary phosphines led to the degradation of the cluster framework and yielded $[(Cp^*Ru)_2(\mu\text{-}H)(\|\text{-}\mu\text{-}\eta^4\text{-}B_2H_5)(PR_3)]$ ($PR_3 = PMe_3$ (**2a**); PMe_2Ph (**2b**)). Thermolysis of **2b** gave the phosphido-bridged complex *nido*-$[(Cp^*Ru)_2(\mu\text{-}PMe_2)(\perp\text{-}\mu\text{-}\eta^4\text{-}B_2H_5)]$ (**3**). The solid-state structures of phosphine complex **2a** and the phosphido-bridged **3** were determined by single-crystal X-ray diffraction. The solid-state structures of these complexes revealed two new modes of coordination for the B_2H_5 fragment. Compound **3** exhibits fluxional behavior in solution.

Introduction

Metallaboranes have attracted much interest because of their structures and bonding.[2−5] It has long been established that the chemistry of metallaboranes parallels that of metal clusters and borane clusters. The relative ease of their syntheses and manipulation is an additional benefit in the study of such compounds. Recently, a number of metallaboranes bearing Cp* (Cp* = pentamethylcyclopentadienyl) ligands, which are good electron donors and are thus effective in stabilizing such complexes, have been synthesized.[5,6]

Our group and that of Fehlner have independently synthesized the complexes *nido*-$[(Cp^*Ru)_2(\mu\text{-}H)_2(B_3H_7)]$ (**1**) and *nido*-$[(Cp^*Ru)_2(\mu\text{-}H)(B_4H_9)]$.[7,8] In reactions with different monoborane reagents, $[Cp^*RuCl]_4$[9] and $[Cp^*RuCl_2]_2$[10] served as sources of the Ru_2 backbone upon which polyborane fragments are assembled under mild conditions.[7,8]

Dimetallaborane clusters, of which a number have been studied,[3−6] are intrinsically interesting due to the novelty that the presence of a metal−metal bond, albeit part of a cluster, can still manifest its flexible metal bonding capabilities. Here we report the borane transformations carried out on a Ru_2 backbone.

Experimental Section

General Comments. All manipulations were carried out under high vacuum or dry nitrogen atmosphere. Reagent-grade hexane and toluene were distilled under nitrogen atmosphere from sodium-benzophenone ketyl, immediately before use. Benzene-d_6 and toluene-d_8 were dried over potassium mirror and transferred before use into NMR tubes. $[(Cp^*Ru)_2(\mu\text{-}H)_2(B_3H_7)]$ (**1**) was prepared according to the literature.[7] NMR spectra were recorded using a JEOL α-500 spectrometer. IR spectra were recorded on a Jasco FTIR-350 spectrometer. Electron impact (EI) mass spectra were obtained using a JEOL JMS-S600H spectrometer. Spectral data of the new complexes are listed in Table 1 (^1H NMR), Table 2 (^{11}B and ^{31}P NMR), and Table 3 (^{13}C NMR and MS).

Synthesis of $[(Cp^*Ru)_2(\mu\text{-}H)(\|\text{-}\mu\text{-}\eta^4\text{-}B_2H_5)(PMe_3)]$ (2a). To a toluene (5 mL) solution of **1** (308 mg, 0.60 mmol) in a Pyrex glass tube equipped with a high-vacuum stopcock was added PMe_3 (91 mg, 1.20 mmol) under vacuum. The solution was stirred for 40 min at −64 °C. After removal of generated $BH_3{\cdot}PMe_3$ and other volatile components, the residue was extracted with hexane (4 mL) and filtered through a glass frit. The hexane extract was allowed to stand at −20 °C to afford $[(Cp^*Ru)_2(\mu\text{-}H)(\|\text{-}\mu\text{-}\eta^4\text{-}B_2H_5)(PMe_3)]$ (**2a**) (187 mg, 0.32 mmol, 54%) as red-orange crystals. Solid **2a** can withstand manipulation in air for short periods of time. Anal. Calcd for $C_{23}H_{45}B_2PRu_2$: C, 47.92; H, 7.87. Found: C, 48.20; H, 7.65. IR (KBr, cm^{-1}): ν(BH) 2453(s), 2386(s); ν(BHB) 2294(m); ν(BHRu) 1991(w), 1913(m); ν(RuHRu) 1810(m).

---

[1] The symbols $\|$ and $\perp$ respectively denote parallel and perpendicular orientation of the B−B axes of the B_2H_5 ligand toward the Ru−Ru bonds.

[2] Fehlner, T. P., Ed. In *Inorganometallic Chemistry*; Plenum: New York, 1992; pp 1−71.

[3] (a) Barton, L.; Srivastava, D. K. In *Comprehensive Organometallic Chemistry II*; Abel, E. W., Stone, F. G. A., Eds.; Pergamon: Oxford, 1995; Vol.1, pp 275−372. (b) Housecroft, C. E. *Polyhedron* **1987**, *6*, 1935. (c) Housecroft, C. E. In *Inorganometallic Chemistry*; Fehlner, T. P., Ed.; Plenum: New York, 1992; pp 73−178.

[4] Fehlner, T. P. *J. Chem. Soc., Dalton Trans.* **1998**, 1525.

[5] For example: (a) Nishihara, Y.; Deck, K. J.; Shang, M.; Fehlner, T. P.; Haggerty, S.; Rheingold, A. L. *Organometallics* **1994**, *13*, 4510. (b) Weller, A. S.; Shang, M.; Fehlner, T. P. *Chem. Commun.* **1998**, 1787. (c) Weller, A. S.; Shang, M.; Fehlner, T. P. *J. Am. Chem. Soc.* **1998**, *120*, 8283. (d) Lei, X.; Shang, M.; Fehlner, T. P. *Organometallics* **1998**, *17*, 1558.

[6] (a) Miller, V. R.; Weiss, R.; Grimes, R. N. *J. Am. Chem. Soc.* **1977**, *99*, 5646. (b) Nishihara, Y.; Deck, K. J.; Shang, M.; Fehlner, T. P. *J. Am. Chem. Soc.* **1993**, *115*, 12224. (c) Aldridge, S.; Shang, M.; Fehlner, T. P. *J. Am. Chem. Soc.* **1998**, *120*, 2586. (d) Ho, J.; Deck, K. J.; Nishihara, Y.; Shang, M.; Fehlner, T. P. *J. Am. Chem. Soc.* **1995**, *117*, 10292. (e) Deck, K. J.; Nishihara, Y.; Shang, M.; Fehlner, T. P. *J. Am. Chem. Soc.* **1994**, *116*, 8408.

[7] Kawano, Y.; Matsumoto, H.; Shimoi, M. *Chem. Lett.* **1999**, 489.

[8] Lei, X.; Shang, M.; Fehlner, T. P. *J. Am. Chem. Soc.* **1999**, *121*, 1275.

10.1021/om000568g CCC: \$19.00
Publication on Web 11/16/2000

Table 1. ^1H NMR Spectral Data for the Diruthenaborane Complexes (500 MHz) δ/ppm

	$[(Cp^*Ru)_2(\mu\text{-}H)(B_2H_5)(PMe_3)]^a$ (**2a**)	$[(Cp^*Ru)_2(\mu\text{-}H)(B_2H_5)(PMe_2Ph)]^a$ (**2b**)	$[(Cp^*Ru)_2(\mu\text{-}PMe_2)(B_2H_5)]^b$ (**3**)
Cp*	1.83 (d, $J_{PH} = 1.5$ Hz, 15H);	1.67 (d, $J_{PH} = 1.5$ Hz, 15H);	1.87 (d, $J_{PH} = 1.0$ Hz, 30H)
	1.88 (s, 15H)	1.90 (s, 15H)	
terminal BH	1.99 (br, 1H);	2.13 (br, 1H);	5.48 (br q $J_{BH} = 190$ Hz, 1H);
	3.15 (br q, $J_{BH} = 85$ Hz, 1H)	3.26 (br, 1H)	−14.09 (br, 3H)
BHB	−2.82 (br, 1H)	−2.68 (br, 1H)	0.52 (br, 1H)
RuHB	−10.93 (q, $J_{BH} = 82$ Hz, 1H);	−10.78 (q, $J_{BH} = 74$ Hz, 1H);	−14.09 (br, 3H)
	−8.45 (q, $J_{BH} = 82$ Hz, 1H)	−8.46 (q, $J_{BH} = 97$ Hz,1H)	
RuHRu	−14.74 (d, $J_{PH} = 21$ Hz, 1H)	−14.67 (d, $J_{PH} = 18$ Hz, 1H)	-
PR_x	1.02 (d, $J_{PH} = 8.5$ Hz, 9H, PMe_3)	1.03 (d, $J_{PH} = 8.0$ Hz, 3H, PMe);	1.32 (d, $J_{PH} = 10.0$ Hz, 3H, PMe)
		1.41 (d, $J_{PH} = 8.5$ Hz, 3H, PMe);	1.49 (d, $J_{PH} = 9.5$ Hz, 3H, PMe)
		7.2−8.0 (m, 5H, PPh)	

[a] The NMR spectra were measured in C_6D_6 at room temperature. [b] The NMR spectra were measured in $C_6D_5CD_3$ at −40 °C.

Table 2. ^{11}B and ^{31}P NMR Spectral Data for the Diruthenaborane Complexes

complex	^{11}B NMR (160 MHz) δ/ppm	^{31}P NMR (202 MHz) δ/ppm
$[(Cp^*Ru)_2(\mu\text{-}H)(B_2H_5)(PMe_3)]^a$ (**2a**)	−4.8, 41.5	18.9
$[(Cp^*Ru)_2(\mu\text{-}H)(B_2H_5)(PMe_2Ph)]^a$ (**2b**)	−4.9, 42.0	32.7
$[(Cp^*Ru)_2(\mu\text{-}PMe_2)(B_2H_5)]^b$ (**3**)	−24.0, 35.1	129.6

[a] The NMR spectra were measured in C_6D_6 at room temperature. [b] The NMR spectra were measured in $C_6D_5CD_3$ at −10 °C.

Synthesis of $[(Cp^*Ru)_2(\mu\text{-}H)(\parallel\text{-}\mu\text{-}\eta^4\text{-}B_2H_5)(PMe_2Ph)]$ (2b). In a similar method used to synthesize **2a**, **1** (308 mg, 0.60 mmol) was reacted with PMe_2Ph (166 mg, 1.20 mmol) at −45 °C for 45 min. Orange crystals of $[(Cp^*Ru)_2(\mu\text{-}H)(\parallel\text{-}\mu\text{-}\eta^4\text{-}B_2H_5)(PMe_2Ph)]$ (**2b**) (130 mg, 0.20 mmol, 34%) were obtained. Solid **2b** can be manipulated in air for short intervals. Anal. Calcd for $C_{28}H_{47}B_2PRu_2$: C, 52.67; H, 7.42. Found: C, 52.39; H, 6.98. IR (KBr, cm^{-1}): ν(BH) 2463(s), 2401(s); ν(BHB) 2365(m); ν(BHRu) 1946(w), 1925(w); ν(RuHRu) 1845(vw).

Synthesis of *nido*-$[(Cp^*Ru)_2(\mu\text{-}PMe_2)(\perp\text{-}\mu\text{-}\eta^4\text{-}B_2H_5)]$ (3). A Pyrex glass tube (15 mm o.d.) was charged with **2b** (130 mg, 0.20 mmol) and toluene (3 mL) and flame-sealed under high vacuum. The solution was kept at 60 °C for 3 days, during which the color of the solution turned from red-orange to bright yellow. The sealed tube was opened in a nitrogen atmosphere glovebox, and the contents were transferred to a Schlenk container. The volatile components of the mixture were removed under vacuum. The residue was extracted with hexane (2 mL) and filtered through cotton plugs. The hexane extract was concentrated and allowed to stand at −20 °C to afford orange crystals (98 mg, 0.18 mmol, 88%) of *nido*-$[(Cp^*Ru)_2(\mu\text{-}PMe_2)(\perp\text{-}\mu\text{-}\eta^4\text{-}B_2H_5)]$ (**3**). Crystalline **3** is quite stable in air. An NMR scale preparation was monitored by multinuclear NMR spectroscopy, and spectral data showed the quantitative conversion of **2b** to **3** with concomitant generation of benzene as a byproduct. Anal. Calcd for $C_{22}H_{41}B_2PRu_2$: C, 47.16; H, 7.38. Found: C, 47.42, H, 7.08%. IR (KBr, cm^{-1}): ν(BH) 2523(s), 2419(s); ν(BHB) 2364(m); ν(BHRu) 1890(m), 1819(m).

X-ray Crystal Structure Determination. Crystals of **2a** and **3** were grown by cooling their hexane solutions. Intensity data were collected using a Rigaku AFC-5 four-circle X-ray diffractometer. Reflection data were corrected for extinction (for **3**) and Lorentz and polarization factors but not for absorption. Space groups were determined from systematic absences. The structures for both crystals were solved by the direct method. For **2a**, the coordinates of hydrogen atoms bound to the boron atoms were determined by difference Fourier synthesis and were refined isotropically. For **3**, similar treatment was applied to the hydrogen atoms bound to boron atoms except for H(12), which bridges B(1) and Ru(2). This particular hydrogen atom was found and fixed. Coordinates of the hydrogen atoms of the methyl groups for both compounds were idealized by using a riding model. Calculations were performed using the programs SHELXS 86[11] and SHELXL 93.[12]

Results and Discussion

Reactions found in this work are outlined in Scheme 1. The square pyramidal *nido*-$[(Cp^*Ru)_2(\mu\text{-}H)_2(B_3H_7)]$ (**1**),[7,8] an analogue of pentaborane(9), undergoes cleavage of the cluster framework through the action of tertiary phosphines. Compounds **2a** and **2b** were obtained in moderate yields from the reaction of **1** with 2 equiv of PMe_3 and PMe_2Ph, respectively. The reaction was initiated through the abstraction of a monoborane fragment to give $BH_3{\cdot}PMe_3$ and $BH_3{\cdot}PMe_2Ph$, respectively, as byproducts. Compounds **2** have 12 skeletal electrons (6 sep) from which a *nido* (tetrahedral) structure is expected for the metallaborane framework. However, complex **2** proved to possess a more opened (spread out) structure (see later). Prolonged interaction between **2a** and excess PMe_3 affords $Cp^*Ru(PMe_3)_2H$.[10a] Note that the reaction of the parent borane, *nido*-B_5H_9, with excess PMe_3 results in the borane fragmentation into $B_2H_4{\cdot}2PMe_3$ and $B_3H_5{\cdot}3PMe_3$ through the 1:2 adduct, $B_5H_9{\cdot}2PMe_3$.[13] Thus, the cleavage of **1** and *nido*-B_5H_9 with phosphines proceeds in different ways.

Thermolysis of **2b** (60 °C in toluene) produced a phosphido-bridged complex *nido*-$[(Cp^*Ru)_2(\mu\text{-}PMe_2)(\perp\text{-}\mu\text{-}\eta^4\text{-}B_2H_5)]$ (**3**), which possesses a tetrahedral metallaborane core, with accompanying liberation of one molecule of benzene from the PMe_2Ph substituent. The activation of P−C bonds, which results in the elimination of phenyl groups as benzene with concurrent formation of bridging μ_2-phosphido or μ_3-phosphinidene functionalities, is ascertained and documented in the reactions of substituted transition metal clusters.[14] The conversion of **2b** to **3** is quantitative, as evidenced by NMR spectroscopy. Remarkably, the B_2H_5 ligand is transformed from the parallel $\mu\text{-}\eta^4$ coordination to the perpendicular $\mu\text{-}\eta^4$ fashion toward the Ru−Ru axis with B→B′ migration of one hydrogen atom. Compound **3** can

---

(9) Fagan, P. J.; Ward, M. D.; Calabrese, J. C. *J. Am. Chem. Soc.* **1989**, *111*, 1698.

(10) (a) Tilley, T. D.; Grubbs, R. H.; Bercaw, J. E. *Organometallics* **1984**, *3*, 274. (b) Oshima, N.; Suzuki, H.; Moro-oka, Y. *Chem. Lett.* **1984**, 1161.

(11) Sheldrick, G. M. *SHELXS-86.* Program for Crystal Structure Determination; University of Göttingen: Göttingen, Germany, 1986.

(12) Sheldrick, G. M. *SHELXL-93.* Program for the Refinement of Crystal Structure; University of Göttingen: Göttingen, Germany, 1993.

(13) Kameda, M.; Kodama, G. *Inorg. Chem.* **1980**, *19*, 2288.

(14) (a) Adams, R. D.; Horváth, I. T. *Prog. Inorg. Chem.* **1985**, *33*, 127. (b) Feilong, J.; Fehlner, T. P.; Rheingold, A. L. *Angew. Chem., Int. Ed. Engl.* **1988**, *27*, 424.

Table 3. ^{13}C NMR and Mass Spectral Data for the Diruthenaborane Complexes

complex	^{13}C NMR (125.7 MHz) δ/ppm	MS (EI) m/z
$[(Cp^*Ru)_2(\mu\text{-H})(B_2H_5)(PMe_3)]^a$ (**2a**)	11.4, 12.6 (C_5Me_5), 19.7 (d, J_{PC} = 29.0 Hz, PMe_3), 82.6 (C_5Me_5), 92.2 (d, J_{PC} = 2.0 Hz, C_5Me_5)	574 (100, $M^+ - 2H$), 486 (40, $M^+ - PMe_3 - BH_3$)
$[(Cp^*Ru)_2(\mu\text{-H})(B_2H_5)(PMe_2Ph)]^a$ (**2b**)	10.9, 12.5 (C_5Me_5), 15.7 (d, J_{PC} = 30.0 Hz, PMe), 20.1 (d, J_{PC} = 29.0 Hz, PMe), 82.9 (C_5Me_5), 92.1 (d, J_{PC} = 2.0 Hz, C_5Me_5), 131–132 (m, PPh)	638 (75, M^+), 635 (94, $M^+ - 3H$), 620 (100, $M^+ - 3H - CH_3$), 558 (51, $M^+ - 3H - Ph$), 497 (45, $M^+ - 3H - PMe_2Ph$), 486 (49, $Cp^*_2Ru_2BH_3^+$)
$[(Cp^*Ru)_2(\mu\text{-PMe}_2)(B_2H_5)]^b$ (**3**)	12.1 (C_5Me_5), 18.9 (d, J_{PC} = 19.0 Hz, PMe), 27.0 (d, J_{PC} = 20.0 Hz, PMe), 92.5 (d, J_{PC} = 2.0 Hz, C_5Me_5)	560 (87, M^+), 558 (100, $M^+ - 2H$), 545 (23, $M^+ - CH_3$), 533 (16, $M^+ - B_2H_5$), 530 (18, $M - 2CH_3$)

[a] The NMR spectra were measured in C_6D_6 at room temperature. [b] The NMR spectra were measured in $C_6D_5CD_3$ at room temperature.

Scheme 1

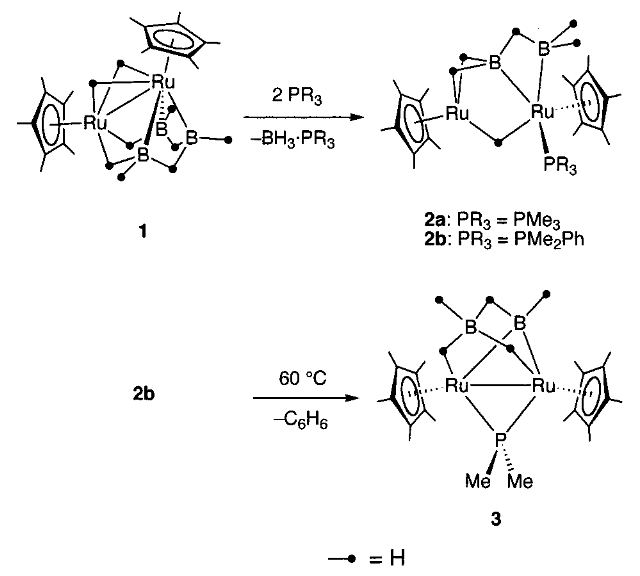

be considered as an analogue of a transient species which can be observed in mass spectroscopy, *nido*-cluster tetraborane(8), B_4H_8 (6 sep).[15]

Characterization of the new complexes was accomplished by NMR, IR, and mass spectroscopy, elemental analysis, and single-crystal X-ray diffraction (for **2a** and **3**). The latter method unequivocally established the two new modes of coordination for the B_2H_5 fragment. The crystal data for **2a** and **3** are summarized in Table 4.

Table 4. Crystal Data for 2a and 3

	2a	**3**
sample	$[(Cp^*Ru)_2(\mu\text{-H})(B_2H_5)(PMe_3)]$	$[(Cp^*Ru)_2(\mu\text{-PMe}_2)(B_2H_5)]$
formula	$C_{23}H_{45}B_2PRu_2$	$C_{22}H_{41}B_2PRu_2$
fw	576.38	560.34
color of cryst	red-orange	orange
temp/°C	20	−5
cryst syst	monoclinic	monoclinic
space group	$P2_1/n$	$C2/c$
systematic absence	$(h,0,l)$: $h + l$; $(0,k,0)$: k	(h,k,l): $h + k$; $(h,0,l)$: l
a/Å	13.850(2)	18.854(2)
b/Å	17.849(1)	15.238(3)
c/Å	10.7815(8)	17.855(3)
β/deg	94.392(7)	101.26(2)
V/Å^3	2657.5(4)	5030.8(1)
Z	4	8
d_{calcd}/g·cm^{-3}	1.441	1.487
μ(Mo Kα)/mm^{-1}	1.186	1.251
cryst size	0.30 × 0.25 × 0.10	0.3 × 0.3 × 0.4
radiation	Mo Kα (λ/Å = 0.71069)	
monochromator	graphite	
reflns measd	$+h,+k,\pm l$	$+h,+k,\pm l$
2θ range/deg	3–55	3–60
scan mode	$2\theta-\omega$	$2\theta-\omega$
ω-scan width/deg	$1.1 + 0.3 \tan\theta$	$1.1 + 0.3 \tan\theta$
ω-scan rate/deg min^{-1}	4.0	4.0
no. of unique data	4244	5379
no. of data used	4111 with $\lvert F_o\rvert > 3\sigma(F_o)$	5268 with $\lvert F_o\rvert > 3\sigma(F_o)$
no. of params refined	303	368
R	0.040	0.052
wR2	0.092	0.167
GooF	1.027	0.233
max resid electron density/Å^3	0.90	1.06

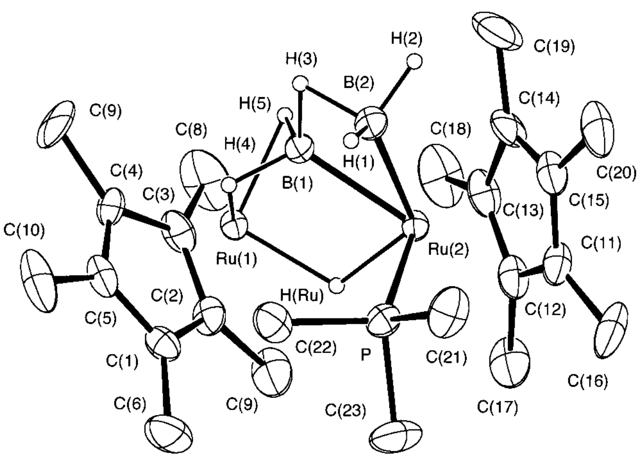

Figure 1. Crystal structure of $[(Cp^*Ru)_2(\mu\text{-H})(PMe_3)(\|\text{-}\mu\text{-}\eta^4\text{-}B_2H_5)]$ (**2a**) with thermal ellipsoids at 30% probability.

Structure of $[(Cp^*Ru)_2(\mu\text{-H})(\|\text{-}\mu\text{-}\eta^4\text{-}B_2H_5)(PMe_3)]$ (2a). Figure 1 shows the molecular structure of **2a**. The key geometric parameters are given in Table 5. Metal centers Ru(1) and Ru(2) are bridged by a hydrido ligand. The B_2H_5 ligand is bound to Ru(2) via a closed BBRu 3c2e bond, while the two hydrogen atoms on B(1) coordinate to Ru(1) through Ru−H−B bonds (Figure 3a). These latter bridging hydrogen atoms, H(4) and H(5), occupy inequivalent positions, as can be inferred from the ^{1}H NMR spectra and from the molecular structure. The three-membered rings of Ru(1)−Ru(2)−B(1) and Ru(2)−B(1)−B(2) are nearly coplanar. The dihedral angle between them is 165.9°. This value is much wider than the corresponding angle in *arachno*-B_4H_{10} (125.5° by electron diffraction;[16] 117.4° by electron diffraction and microwave spectroscopy[17]) and reported *arachno*-dimetallaboranes (e.g., $[Cp^*_2Ir_2H_3(B_2H_5)]$,[18] 115.8°; $[\{(OC)_4Cr\}_2(\eta^4\text{-}H,H',H'',H'''\text{-}BH_2BH_2\cdot PMe_2CH_2PMe_2)]$,[19] 130.3°), despite the number of skeletal electrons of 12 for compound **2**, from which a *nido* structure

---

(15) Hollins, R. E.; Stafford, F. E. *Inorg. Chem.* **1970**, *9*, 877.
(16) Nordman, C. E.; Lipscomb, W. N. *J. Chem. Phys.* **1953**, *21*, 1856.
(17) Dain, C. J.; Downs, A. J.; Laurenson, G. S.; Rankin, D. W. H. *J. Chem. Soc., Dalton Trans.* **1981**, 472.

Table 5. Key Geometric Parameters for $[(Cp^*Ru)_2(\mu\text{-}H)(B_2H_5)(PMe_3)]$ (2a)

Distances (Å)			
Ru(1)−Ru(2)	3.008(1)	Ru(1)−B(1)	2.304(6)
Ru(2)−B(1)	2.136(6)	Ru(2)−B(2)	2.241(6)
Ru(2)−P	2.258(2)	Ru(1)−H(4)	1.83(5)
Ru(1)−H(5)	1.66(5)	B(1)−H(4)	1.36(5)
B(1)−H(5)	1.23(5)	B(2)−H(1)	1.15(5)
B(2)−H(2)	1.13(6)	B(1)−H(3)	1.24(5)
B(2)−H(3)	1.34(5)	B(1)−B(2)	1.733(9)
Ru(1)−H(Ru)	1.851(7)	Ru(2)−H(Ru)	1.715(7)
Angles (deg)			
Ru(1)−B(1)−Ru(2)	92.3(2)	B(1)−Ru(2)−B(2)	46.6(2)
Ru(1)−Ru(2)−P	95.35(4)	B(1)−Ru(1)−Ru(2)	45.2(2)
Ru(1)−Ru(2)−B(1)	42.5(2)	H(4)−B(1)−H(5)	100(3)

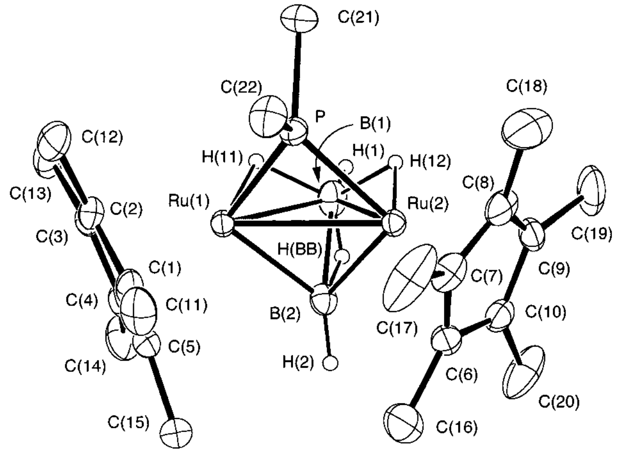

Figure 2. Crystal structure of $[(Cp^*Ru)_2(\mu\text{-}PMe_2)(\perp\text{-}\mu\text{-}\eta^4\text{-}B_2H_5)]$ (**3**) with thermal ellipsoids at 30% probability.

is expected. The bond length between Ru(2) and the boron atom at the bridging position, B(1) (2.136(6) Å), is substantially shorter than that between Ru(2) and B(2) (2.241(6) Å). Similar phenomena have been observed in related cobalt and platinum complexes, $[Cp_2Co_2(\mu\text{-}PPh_2)(\mu\text{-}\eta^3\text{-}B_2H_5)]$[20] and $[(B_6H_9)Pt_2(PMe_2Ph)_2(\mu\text{-}\eta^3\text{-}B_2H_5)]$.[21] The interatomic distance between Ru(1) and Ru(2) (3.008(1) Å) is near the longer limit of reported Ru−Ru single bond distances.[22]

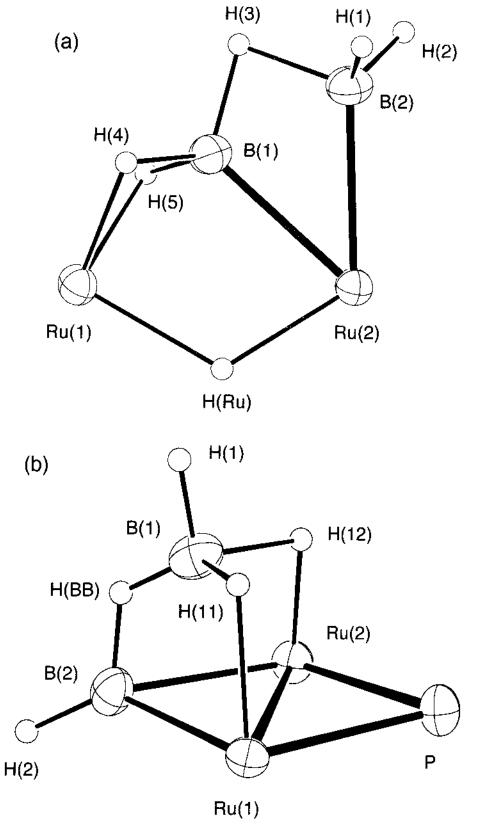

Figure 3. Core structures of (a) $[(Cp^*Ru)_2(\mu\text{-}H)(PMe_3)(\|\text{-}\mu\text{-}\eta^4\text{-}B_2H_5)]$ (**2a**) and (b) $[(Cp^*Ru)_2(\mu\text{-}PMe_2)(\perp\text{-}\mu\text{-}\eta^4\text{-}B_2H_5)]$ (**3**).

Table 6. Key Geometric Parameters for $[(Cp^*Ru)_2(\mu\text{-}PMe_2)(B_2H_5)]$ (3)

Distances (Å)			
Ru(1)−Ru(2)	2.802(1)	Ru(1)−B(1)	2.259(9)
Ru(1)−B(2)	2.140(8)	Ru(2)−B(1)	2.270(8)
Ru(2)−B(2)	2.152(8)	B(1)−B(2)	1.73(1)
Ru(1)−P	2.267(2)	Ru(2)−P	2.270(2)
Ru(1)−H(11)	1.785(1)	Ru(2)−H(12)	1.420(1)
B(1)−H(11)	1.354(9)	B(1)−H(12)	1.505(9)
B(1)−H(1)	1.038(9)	B(2)−H(2)	1.028(8)
B(1)−H(BB)	0.938(8)	B(2)−H(BB)	1.027(8)
Ru(1)−Cp*(1)	1.888(1)	Ru(2)−Cp*(2)	1.886(1)
Angles (deg)			
Ru(1)−B(1)−Ru(2)	76.5(3)	Ru(1)−B(1)−B(2)	63.3(3)
Ru(1)−B(2)−Ru(2)	81.5(3)	B(1)−Ru(1)−B(2)	46.2(3)
B(1)−Ru(2)−B(2)	46.0(3)	Ru(2)−B(1)−B(2)	63.4(4)
Ru(1)−B(2)−B(1)	70.5(4)	Ru(2)−B(2)−B(1)	70.6(4)
B(1)−Ru(1)−Ru(2)	52.0	B(2)−Ru(1)−Ru(2)	49.4
B(1)−Ru(2)−Ru(1)	51.6	B(2)−Ru(2)−Ru(1)	49.1
Ru(1)−P−Ru(2)	76.26(6)		

Structure of *nido*-$[(Cp^*Ru)_2(\mu\text{-}PMe_2)(\perp\text{-}\mu\text{-}\eta^4\text{-}B_2H_5)]$ (3). Figure 2 shows the molecular structure of complex **3**, and Table 6 lists its key geometric parameters. The three-membered rings composed of P−Ru(1)−Ru(2) and Ru(1)−Ru(2)−B(2) are almost coplanar, with a dihedral angle of 173.1°. B(1) is located on top of the tetrahedron with the latter triangle as the base (Figure 3b). The two Cp* ligands are mutually cis and positioned opposite B(1) with respect to the P−Ru(1)−B(2)−Ru(2) four-membered ring. The two ruthenium atoms have essentially identical environments, and the B_2H_5 fragment is oriented perpendicularly to the Ru−Ru axis. The intermetallic distance measures 2.802(1) Å, which is within the range of regular Ru−Ru single bonds. The metal centers are also bridged by a tetrahedral dimethylphosphido group with an average Ru−P distance of 2.269 Å and Ru(1)−P−Ru(2) angle of 76.26(6)°. The latter value is consistent with phosphido groups bridging singly bonded metal centers.[23] B(1)−Ru(1) and B(1)−Ru(2) linkages are each bridged by a hydrogen atom and display an average distance of 2.265 Å, which is approximately 0.12 Å longer than the average distance of B(2) from the metal centers (av 2.146 Å).

---

(18) (a) Lei, X.; Bandyopadhyay, A. K.; Shang, M.; Fehlner, T. P. *Organometallics* **1999**, *18*, 2294. (b) Lei, X.; Shang, M.; Fehlner, T. P. *Chem. Eur. J.* **2000**, *6*, 2653.

(19) Hata, M.; Kawano, Y.; Shimoi, M. *Inorg. Chem.* **1998**, *37*, 4482.

(20) Feilong, J.; Fehlner, T. P.; Rheingold, A. L. *J. Organomet. Chem.* **1988**, *348*, C22.

(21) Ahmad, R.; Crook, J. E.; Greenwood, N. N.; Kennedy, J. D.; McDonald, W. S. *J. Chem. Soc., Chem. Commun.* **1982**, 1019.

(22) Examples of complexes with long Ru−Ru bond distances: (a) $[Ru_2H(CO)_4(Ph_2PCHPPh_2)\{PhPC_6H_4C(O)\}]$ (2.972(1) Å): Clucas, J. A.; Harding, M. M.; Nicholls, B. S.; Smith, A. K. *J. Chem. Soc., Dalton Trans.* **1985**, 1835. (b) $[\{Cp^*Ru(\mu\text{-}\eta^2\text{-}HSiEt_2)\}_2(\mu\text{-}H)(H)]$ (2.971(1) Å): Suzuki, H.; Takao, T.; Tanaka, M.; Moro-oka, Y. *Chem. Soc., Chem. Commun.* **1992**, 476. (c) $[Ru_2(\mu\text{-}PPh_2CH_2SiMe_2)_2(CO)_6]$ (3.056(1) Å): Auburn, M. J.; Holmes-Smith, R. D.; Stobart, S. R.; Zaworotko, M. J.; Cameron, T. S.; Kumari, A. *Chem. Soc., Chem. Commun.* **1983**, 1523.

(23) (a) Carty, A. J. *Adv. Chem. Ser.* **1982**, *196*, 163. (b) Garrou, P. E. *Chem. Rev.* **1981**, *81*, 229.

Solution Behavior of 2 and 3. In the ^{1}H NMR spectra of compounds **2a** and **2b**, both complexes exhibited a sharp singlet and a doublet (due to coupling to phosphorus) for the Cp* ligands. The two terminal B*H* protons are observed separately because of inequivalent environment (**2a**, 1.99 and 3.15 ppm; **2b**, 2.13 and 3.26 ppm). The signal at 3.15 ppm for **2a** gave a coupling constant, J_{BH} = 85 Hz, which is lower than regular values of coupling due to a terminal B*H*,[24] but is close to that of a dicobaltaborane with a related structure, $[(CpCo)_2(\mu\text{-}PPh_2)(\mu\text{-}\eta^3\text{-}B_2H_5)]$ (ca. 90 Hz).[20] Ru*H*B peaks for **2a** (−8.45 and −10.93 ppm) and **2b** (−8.46 and −10.78 ppm) appear as broad quartets with an equal integration of one. The signals for B*H*B in **2a** (−2.82 ppm) and **2b** (−2.68 ppm) appear as broad humps for both complexes. Sharp doublet peaks (coupled to phosphorus) were assigned to Ru*H*Ru for **2a** (−14.74 ppm) and **2b** (−14.67 ppm). The high-field values for bridging hydrides indicate that these protons experience particularly strong shielding from the metal centers. For both compounds, the ^{11}B NMR spectra showed two peaks of equal intensity: **2a** (−4.8 and 41.5 ppm) and **2b** (−4.9 and 42.0 ppm). Peaks at the lower field were assigned to the boron atom which bridges the two ruthenium metals. This assignment is in agreement with the low-field ^{11}B NMR resonances of boron atoms directly bound to metal centers (no B−H−M bridges) in *μ*-borylene complexes[25,26] and in metallaborane clusters[5a,14b,27] and that of ^{13}C NMR shifts for *μ*-carbene complexes.[28]

The proton-decoupled ^{11}B NMR spectrum of complex **3** showed two broad peaks of equal intensity (35.1 and −24.0 ppm). The signal at lower field is assigned to the borylidene (BH) unit. This designation is similarly based on the observed low-field shift in the ^{11}B NMR spectra of complexes with direct B−M bonds and ^{13}C NMR spectra of *μ*-carbene complexes.[5a,14b,25−28] Low-temperature nondecoupled ^{11}B NMR measurements gave a broad doublet for the borylidene (BH) boron (J_{BH} = 130 Hz) and a broad peak for the BH_4 unit at 34.9 and at −24.3 ppm, respectively. For the latter, no BH coupling was observed due to fluxionality (see later). The low-field-shifted signal in the ^{31}P NMR (129.6 ppm) is consistent with the existence of a phosphido group in **3**.[23] Unlike its precursor **2b**, the ^{1}H NMR spectra of **3** gave one doublet (coupling to phosphorus) for two Cp* fragments at 1.87 ppm. The ^{1}H NMR spectrum of **3** shows three B*H* protons at 5.48, 0.52, and −14.09 ppm in 1:1:3 ratio at room temperature. The broad hump at 0.5 ppm is assigned to the B*H*B proton. The chemical shift value of 5.48 ppm is close to that of the B*H* proton of a *μ*-borylene dicobalt complex, $[Co_2(CO)_6(\mu\text{-}CO)(\mu\text{-}BH\cdot PMe_3)]$,[25] and attributed to the terminal hydrogen attached to B(2) (see Figure 2). The third signal with 3H integration (−14.09 ppm) is assignable to the averaged signal of the terminal hydrogen and B*H*Ru hydrogen atoms on B(1). Scrambling of these protons can occur by the rotation of the BH_3 fragment about the B(1)−H_d (bridging) axis (Scheme 2, process I).[29] The activation energy for this process can be estimated to be less than 35 kJ mol^{-1} at −60 °C, on the assumption that the original chemical shift values of the terminal and metal-coordinated B*H*'s are 0 and −21 ppm, respectively, since this signal shows no sign of decoalescence at this temperature. This value of $\Delta G^{\ddagger}$ is considerably smaller than that for the related fluxional process of a diiron anion, $[Fe_2(CO)_6(B_2H_5)]^-$.[29] In this anion, the BH_2 fragment is rotated around a B−H (bridging) axis, thereby causing the terminal and B*H*Fe protons to be averaged (Scheme 3). However, coalescence of the protons of this anion is not observed up to 50 °C at 300 MHz.

At higher temperature, another fluxional process is observed for complex **3** (Figure 4). The two methyl groups attached to phosphorus show separated doublets (1.49 and 1.32 ppm) at −10 °C. As the temperature is raised to 32 °C, they coalesced into one broad peak. Further increase in temperature results in sharpening of the PMe_2 peak into a doublet. These observations indicate the existence of a dynamic process which makes both sides of the P−Ru(1)−Ru(2) three-membered ring equivalent. Above 60 °C, the signal of the terminal hydrogen on B(2) (5.48 ppm) collapsed into the baseline and the signal at −14.09 ppm also partially collapsed. It indicates that the averaging of terminal and Ru*H*B protons on B(1) and the terminal proton on B(2) is occurring. Moreover, the two peaks in the ^{11}B NMR spectrum collapsed with signs of converging at this temperature, although the coalesced signal was not observed up to 110 °C. A plausible mechanism that can explain these observations is shown in Scheme 2. The metal-coordinated B*H*Ru protons transfer to the adjacent RuB edges in the borylidene unit. Attendant flip-flopping of the phosphido and Cp* groups accompanies this process to yield the equivalent structure. It is difficult to explain the edge-to-edge hydrogen transfer by rotation of a boron moiety around any axis; we therefore propose simple migration of the hydrogen atoms across Ru−B−B′ faces (Scheme 2, process II). A metallaborane compound with face-bridging hydrogen atoms was recently reported.[18] The energy of activation for process II is estimated to be approximately 60 kJ mol^{-1} at 305 K. In the form generated by this process, BH_3 rotation about the B(2)−H_d axis causes exchange of terminal BH on B(2) and Ru*H*B protons (process I′). Through processes I, I′, and II, scrambling of all B*H* protons except B*H*B is achieved. Selective decoupling

---

[24] Examples of compounds containing the B_2H_5 fragment that exhibited resolved coupling for the terminal B*H*: $K[(CO)_4M(B_2H_5)]$ δ 1.80 (J_{BH} = 112 Hz, M = Fe), 1.56 (J_{BH} = 100 Hz, M = Ru), 1.45 (J_{BH} = 116 Hz, M = Os); $[CpM(CO)_2(B_2H_5)]$ δ 5.01 (J_{BH} = 117 Hz, M = Fe), 5.39 (J_{BH} = 119 Hz, M = Ru). Coffy, T. J.; Medford, G.; Plotkin, J. S.; Long, G. J.; Huffman, J. C.; Shore, S. G. *Organometallics* **1989**, *8*, 2404.

[25] Shimoi, M.; Ikubo, S.; Kawano, Y.; Katoh, K.; Ogino, H. *J. Am. Chem. Soc.* **1998**, *120*, 4222.

[26] (a) Braunschweig, H.; Wagner, T. *Angew. Chem., Int. Ed. Engl.* **1995**, *34*, 825. (b) Braunschweig, H.; Müller, M. *Chem. Ber.* **1997**, *130*, 1295. (c) Braunschweig, H.; Kollann, C.; Englert, U. *Angew. Chem., Int. Ed.* **1998**, *37*, 3179. (d) Braunschweig, H.; Kollann, C.; Englert, U. *Eur. J. Inorg. Chem.* **1998**, 465. (e) Braunschweig, H.; Kollann, C.; Klinkhammer, K. W. *Eur. J. Inorg. Chem.* **1999**, 1523.

[27] Lei, X.; Shang, M.; Fehlner, T. P. *Inorg. Chem.* **1998**, *37*, 3900.

[28] For examples of *μ*-carbene compounds see: (a) Holton, J.; Lappert, M. F.; Pearce, R.; Yarrow, P. I. W. *Chem. Rev.* **1983**, *83*, 135. (b) Bruce, M. I. *Chem. Rev.* **1991**, *91*, 197. (c) Takusagawa, F.; Fumagalli, A.; Koetzle, T. F.; Herrmann, W. A. *Inorg. Chem.* **1981**, *20*, 3060. (d) Dyke, A. F.; Knox, S. A. R.; Naish, P. J.; Taylor, G. E. *J. Chem. Soc., Dalton Trans.* **1982**, 1297. (e) Dyke, A. F.; Knox, S. A. R.; Morris, M. J.; Naish, P. J. *J. Chem. Soc., Dalton Trans.* **1983**, 1417. (f) Orpen, A. G. *J. Chem. Soc., Dalton Trans.* **1983**, 1427. (g) Matsuzaka, H.; Mizobe, Y.; Nishio, M.; Hidai, M. *J. Chem. Soc., Chem. Commun.* **1991**, 1011.

[29] Fehlner has suggested that the BH_3 group does not rotate for $[Fe_2(CO)_6(B_2H_6)]$. Jacobsen, G. B.; Andersen, E. L.; Housecroft, C. E.; Hong, F.-E.; Buhl, M. L.; Long, G. J.; Fehlner, T. P. *Inorg. Chem.* **1987**, *26*, 4040.

Scheme 2. I: BH_3 Rotation around the B1−H_d Axis. I′: BH_3 Rotation around the B2−H_d Axis. II: Migration of the Ru−H−B Protons through the BB′Ru Faces

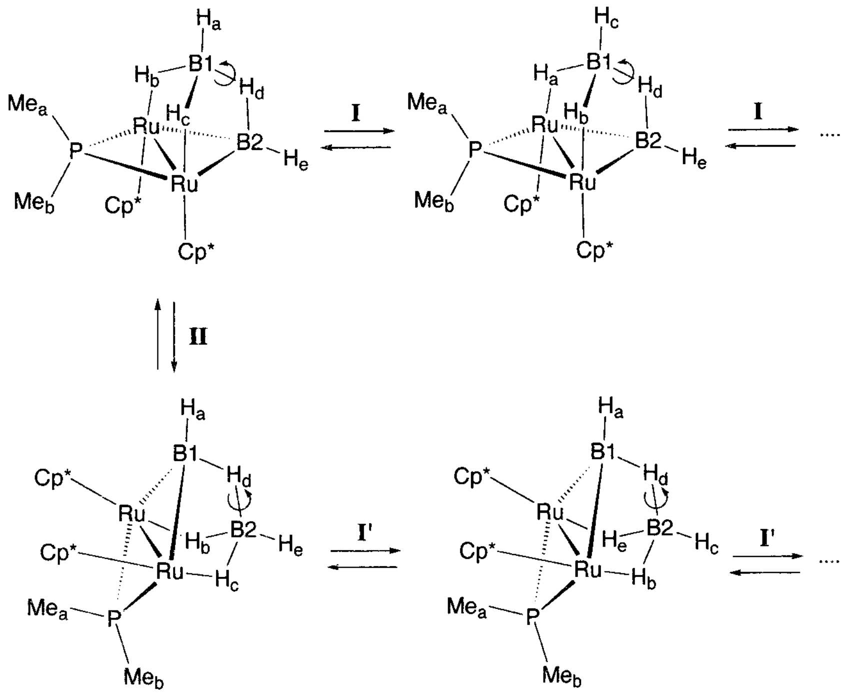

Scheme 3. Fluxional Behavior of $Fe_2(CO)_6(B_2H_5)^-$

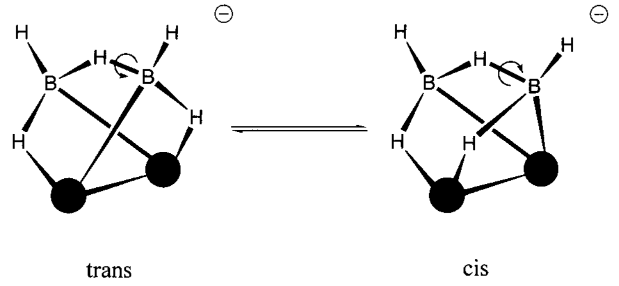

experiments confirm the aforementioned mechanism: irradiation of the ^1H signal at −14.09 (Ru*H*B and a terminal *H*) and at 5.48 ppm (terminal *H*) at 35 °C affects both boron signals alike; at −15 °C, where no hydrogen exchange between B(1) and B(2) occurs, changes in ^{11}B NMR signals were detected upon irradiation of respective protons associated with individual boron centers.

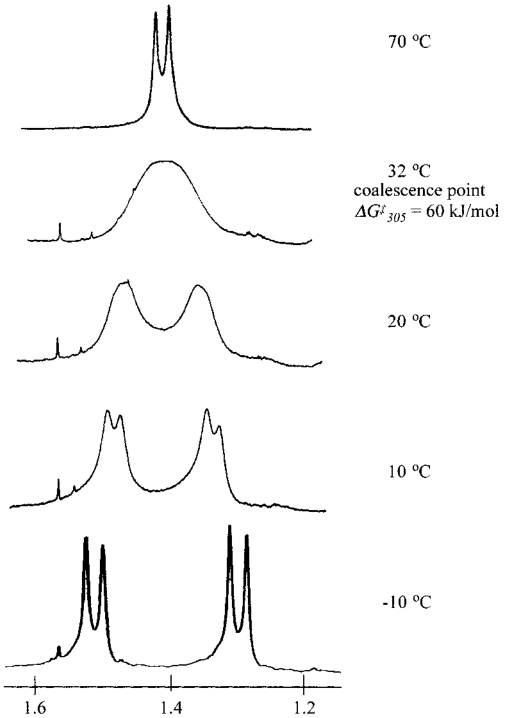

Figure 4. PMe_2 region in the ^1H NMR spectra of **3**.

B_2H_5 Fragment. $B_2H_5^-$ is isoelectronic with ethylene and is one of the fundamental ligands in metallaborane chemistry. Figure 5 summarizes the crystallographically confirmed modes of coordination for B_2H_5. The B_2H_5 group of **2a** coordinates to the diruthenium moiety in an unprecedented parallel μ-η^4-mode (**A**) possessing two Ru−H−B interactions and a closed BBRu 3c2e bond. The bidentate coordination for the B_2H_5 ligand to a mononuclear metal center (**C**) is most commonly encountered, e.g., $[Cp_2MoH(\eta^2\text{-}B_2H_5)]$,[30] $[CpM(CO)_2(\eta^2\text{-}B_2H_5)]$ (M = Fe, Ru),[24,31] $K[M(CO)_4(\eta^2\text{-}B_2H_5)]$ (M = Fe, Ru, Os),[24,31] and $[MH(CO)_4(\eta^2\text{-}B_2H_5)]$ (M = Ru, Os).[32] In these complexes, the metal fragment is viewed as a replacement of a bridging hydrogen in diborane(6). Another type of attachment is demonstrated by the asymmetrically bridging μ-η^3-B_2H_5 fragment (**D**). It is present in $[Cp_2Co_2(\mu\text{-}PPh_2)(\mu\text{-}\eta^3\text{-}B_2H_5)]$,[20] $[(B_6H_9)Pt_2(PMe_2Ph)_2(\mu\text{-}\eta^3\text{-}B_2H_5)]$,[21] and $[Cp^*_2Ir_2H_3(\mu\text{-}\eta^3\text{-}B_2H_5)]$.[18] These complexes exhibit one M*H*B bond. These compounds similarly possess the closed BBM 3c2e bonds. Further, the metal-rich metallaborane cluster $[HRu_3(CO)_9(\mu\text{-}\eta^4\text{-}$

---

(30) Grebenik, P. D.; Green, M. L. H.; Kelland, M. A.; Leach, J. B.; Mountford, P.; Stringer, G.; Walker, N. M.; Wong, L.-L. *J. Chem. Soc., Chem. Commun.* **1988**, 799.

(31) (a) Medford, G.; Shore, S. G. *J. Am. Chem. Soc.* **1978**, *100*, 3953. (b) DeKock, R. L.; Deshmukh, P.; Fehlner, T. P.; Housecroft, C. E.; Plotkin, J. S.; Shore, S. G. *J. Am. Chem. Soc.* **1983**, *105*, 815. (c) Plotkin, J. S.; Shore, S. G. *J. Organomet. Chem.* **1979**, *182*, C15.

(32) Coffy, T. J.; Shore, S. G. *J. Organomet. Chem.* **1990**, *394*, C27.

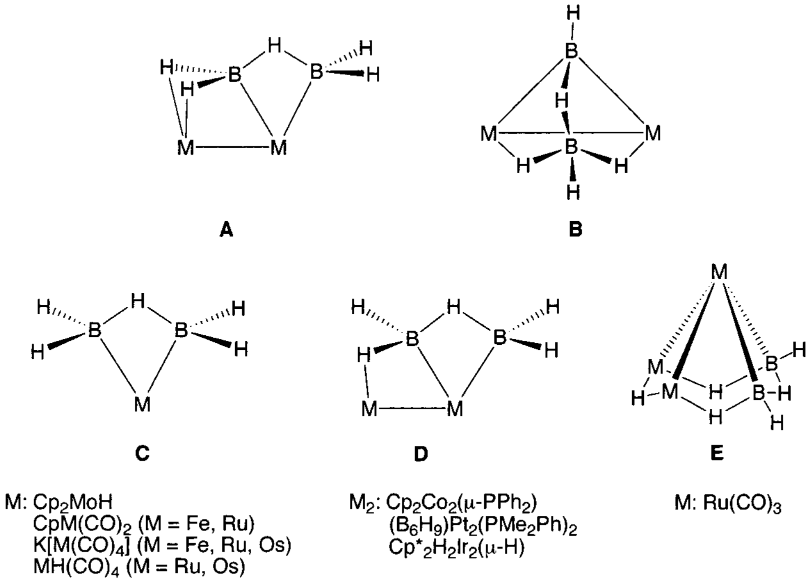

Figure 5. Different modes of coordination for the B_2H_5 ligand.

B_2H_5)][33] and its derivatives also contain a distinct mode of coordination for B_2H_5 over a triruthenium framework (**E**).

Structures related to that of **3** have been postulated from Mössbauer and NMR spectroscopic analyses of $B_2H_6Fe_2(CO)_6$ and its conjugate base, $[B_2H_5Fe_2(CO)_6]^-$.[29] These complexes bear analogous distorted Fe_2B_2 tetrahedra but with a distinct hydrogen distribution/location (Scheme 3). A relevant asymmetric coordination of a B_2H_6 group is also found in $[Cp^*{}_2Ta_2(\mu\text{-Br})_2(B_2H_6)]$.[34] The B_2H_5 ligand in **3** is unique in the asymmetric arrangement. The perpendicular mode of coordination in **3** is characterized by a BH_4 fragment possessing two Ru*H*B interactions and a borylidene B*H* component forming two RuB bonds (**B**).

The thermolytic transformation of **2** to **3** is quite rare for metallaboranes. The $B_2H_5^-$ ligand both in **2** and **3** acts as a six-electron donor. Hence, the skeletal electron count of 12 is kept during the conversion from **2** to **3**. However, by this conversion, the core structure is changed to *nido* (tetrahedron), which is the expected structure from the electron count. The perpendicular orientation of the B_2H_5 ligand in **3** is presumably preferred by the shrunken Ru−Ru bond caused by the deprotonation of the Ru−H−Ru bond and the formation of the phosphido bridge. This transformation is reminiscent of parallel-to-perpendicular conversion of coordinated alkyne ligands in some dinuclear complexes. The dimethylacetylenecarboxylate ligand in a dirhenacyclobutene complex $[\{Cp^*(CO)_2Re\}_2(\mu\text{-}MeO_2CC{\equiv}CCO_2Me)]$[35] becomes perpendicularly coordinated upon photolysis, yielding a dirhenabicyclo[1.1.0]butane (eq 1).

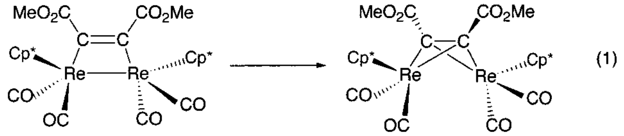

Similarly, the hexafluorobutyne ligand in $[(CO)_4Ru(\mu\text{-}CF_3C{\equiv}CCF_3)Co(CO)Cp^*]$[36] and $[\{Cp(CO)Rh\}_2(\mu\text{-}CF_3C{\equiv}CCF_3)]$[37] changes the mode of coordination from parallel to perpendicular toward the metal−metal axis with loss of CO.

Acknowledgment. This work was supported by a Grant-in-Aid for Scientific Research (No. 11440193) from the Japanese Ministry of Education, Science, Sports and Culture. We also gratefully acknowledge the scholarship granted to L.N.P. from the same agency.

Supporting Information Available: Full listings of crystallographic data, complete atomic coordinates, isotropic and anisotropic thermal parameters, and bond distances and angles for complexes **2a** and **3**. This material is available free of charge via the Internet at http://pubs.acs.org.

OM000568G

---

[33] (a) Chipperfield, A. K.; Housecroft, C. E.; Matthews, D. M. *J. Organomet. Chem.* **1990**, *384*, C38. (b) Housecroft, C. E.; Matthews, D. M.; Rheingold, A. L. *J. Chem. Soc., Chem. Commun.* **1992**, 323. (c) Housecroft, C. E.; Matthews, D. M.; Edwards, A. J.; Rheingold, A. L. *J. Chem. Soc., Dalton Trans.* **1993**, 2727.

[34] Ting, C.; Messerle, L. *J. Am. Chem. Soc.* **1989**, *111*, 3449.

[35] Casey, C. P.; Cariño, R. S.; Hayashi, R. K.; Schladetzky, K. D. *J. Am. Chem. Soc.* **1996**, *118*, 1617.

[36] Gagne, M. R.; Takats, J. *Organometallics* **1988**, *7*, 561.

[37] Dickson, R. S.; Pain, G. N. *J. Chem. Soc., Chem. Commun.* **1979**, 277.